Structural Health Monitoring of Wind Turbine Blades

A Diagnostic Study of Structural Anomalies and Failure Detection in Rotor Blades

Raonak Shukla

November 17, 2025

Executive Summary

A Blade Condition Monitoring System was used to evaluate the structural health and dynamic performance of three 62-m wind turbine blades across two data collections, taken six months apart. Each blade is instrumented with accelerometers at the root and tip, enabling detailed analysis of vibration behaviour in the flapwise, edgewise, and spanwise directions. The objective of the analysis was to determine whether the blades exhibit normal structural and dynamic behaviour and to identify early-stage or developing defects. Across all analytical methods time-domain statistics, spectral analysis (Welch PSD), coherence, transmissibility, Frequency Domain Decomposition (FDD), Stochastic Subspace Identification (SSI), and Modal Assurance Criterion (MAC), the results consistently demonstrate that **Turbine 1 is dynamically healthy**, while **Turbine 2 exhibits clear, measurable signs of structural degradation**, with the most severe issues detected on **Blade 3**.

Key findings include the following:

- Turbine 2 exhibits **significantly higher broadband vibration energy** (1–30 Hz) across all axes, especially in flapwise tip channels, indicating increased loading or reduced stiffness.
- The first flapwise natural frequency is reduced by **7–8%** for all Turbine 2 blades, a strong indicator of global stiffness loss or mass increase due to degradation.
- Turbine 2 shows **elevated damping ratios** (up to an order of magnitude higher), consistent with internal friction caused by cracking, delamination, or deteriorating adhesive joints.
- Coherence analysis reveals **degraded root–tip coherence and abnormal coupling at the tip**, suggesting compromised load-transfer pathways and potential trailing-edge or spar-cap damage.
- Transmissibility is **elevated**, especially in flapwise and spanwise directions, matching the signature of stiffness loss along the spar cap or shear web.

- MAC analysis confirms the severity of the issue: Blade 1 of Turbine 2 is mostly healthy, Blade 2 shows moderate stiffness changes, and **Blade 3 shows severe modal deformation (MAC ≈ 0 for Mode 3)**, indicating a fundamental structural abnormality.

Collectively, these observations strongly indicate that **Blade 3 on Turbine 2 is experiencing significant structural degradation**. Likely mechanisms include spar-cap cracking, trailing-edge separation, shear-web debonding, core/foam delamination, or localized bond-line failure. Because both turbines operated at the same rotor speed during the data collection, the observed differences can be confidently attributed to structural, rather than operational change.

Recommendations

Immediate Actions (Within 1–2 Weeks)

- Perform a targeted inspection of **Blade 3 on Turbine 2** using:
  - UAV high-resolution visual inspection,
  - Thermographic imaging to detect internal delamination,
  - Tap-testing / acoustic methods for spar-cap or web defects,
  - Boroscope inspection where internal access is possible.
- Inspect for trailing-edge cracks and separation between 60–90% span.
- Review pitch-system logs to verify root boundary integrity.

Short-Term Actions (Next 1–3 Months)

- Schedule a blade-internal inspection during the next maintenance window to assess:
  - Spar-cap condition,
  - Shear-web and core integrity,
  - Bond-line adhesion quality,

  - Moisture ingress or accumulated water.
- Implement continuous monitoring of natural frequencies and damping for all blades.
- Verify mass balance to rule out water ingress or uneven surface wear.

Long-Term Actions (3–12 Months)

- Establish a dynamic baseline library and update CMS thresholds for early-warning detection.
- Apply trend-based modal tracking to identify progressive stiffness decline.
- Integrate CMS data with SCADA wind-speed and pitch-angle logs for deeper diagnostics.
- Repeat the full modal analysis after repairs or inspection to confirm structural restoration.

Final Assessment

Turbine 1 remains structurally healthy with stable modal properties and nominal vibration levels. Turbine 2, however, shows **consistent, multi-method evidence of stiffness loss and altered dynamic behaviour—a clear indicator of structural degradation**. The most serious concern is **Blade 3 on Turbine 2**, which requires urgent inspection, followed by Blade 2 for moderate deterioration. Early corrective action is strongly recommended to prevent defect progression and reduce the risk of major blade failure.

Click on the link to access-

Monitoring Dashboard: https://conditionalmonitoring.streamlit.app/

Repository: https://github.com/raonakshukla/Conditional_Monitoring_Wind_Turbine_Blades

Problem Statement

A new Blade Condition Monitoring System (Blade CMS) has been installed on a wind turbine, with each blade instrumented using two tri-axial MEMS accelerometers: one at the blade root and one at the blade tip, or as close to the tip as practically possible. The turbine blades are approximately 62 meters in length, and the CMS records vibration data at a sampling rate of 62.5 Hz in 10-minute bursts.

Using the first several data bursts collected by the system, the task is to process and analyse the accelerometer signals to evaluate the health and dynamic performance of the blades. This includes determining whether the blades exhibit normal behaviour and, if not, diagnosing potential defects such as imbalance, structural damage, or looseness.

Feature Description

The dataset consists of vibration measurements from a Blade Condition Monitoring System installed on a wind turbine, where each blade is instrumented with two tri-axial accelerometers located at the blade root and tip. Each sensor records acceleration in three orthogonal directions: flap, which captures bending perpendicular to the plane of rotation; edgewise, which measures in-plane vibration influenced by drag, torque, and gravity; and span, which measures acceleration along the blade's length. Together, the three axes from the two sensors on each blade generate six channels per blade, resulting in a total of 18 features across all three blades. Two datasets are provided for comparison, collected about six months apart. The sampling frequency is 62.5 Hz, with each measurement run lasting 10 minutes, yielding 37,500 data points per channel in each dataset. For the purposes of this analysis, the dataset *batch_121219* is designated as Turbine 1, while *batch_199672* is designated as Turbine 2.

Data Cleaning and Preparation

Data cleaning is the first essential step in preparing the vibration signals for analysis. The process begins with verifying that the time interval between consecutive samples remains constant, as any irregularity could lead to aliasing and spectral leakage in subsequent frequency-domain analysis. The recorded sampling rate of 62.5 Hz ensures that the data is well above the turbine's rotational frequency, enabling reliable capture of dynamic peaks associated with blade vibration. The measured time step of approximately 16 milliseconds is consistent across all samples in both datasets, confirming uniform sampling.

In the second dataset, a small number of missing values were identified near the end of the recording and were therefore removed from the analysis. If missing values had occurred within the interior of the signal, interpolation would have been applied to reconstruct the data; however, this was unnecessary for the datasets provided. To isolate the vibration content from quasi-static loads and gravitational effects, the signals were detrended and subsequently filtered using a high-pass Butterworth filter with a cutoff frequency of 0.1 Hz. This threshold is selected based on the assumption that the minimum rotor speed is approximately 6 RPM, ensuring the removal of frequencies unrelated to blade vibration dynamics.

Workflow

The analysis begins with descriptive time-domain statistics for each vibration channel, including mean, RMS, standard deviation, skewness, kurtosis, crest factor, impulse factor, clearance factor, and margin factor. These metrics establish the baseline vibration energy, signal variability, and impulsiveness of the response. After the time-domain assessment, the analysis proceeds to the frequency domain, which is essential for identifying resonance behaviour, harmonics, and changes in vibratory energy that may indicate structural defects or increased loading. Welch's Power Spectral Density (PSD) method is used to evaluate

each channel and compare spectral characteristics between the two datasets collected six months apart, noting that variations may arise from operational differences such as wind speed.

Following the PSD evaluation, coherence analysis is performed to assess how different parts of the blade move relative to one another. High coherence between specific DOFs for example, between tip-flap and root-edge can indicate torsional coupling, which may impose additional stresses on adhesive joints such as the spar-cap–shear-web interface. Coherence values are quantified at the 1P (rotational) frequency for all relevant sensor pairs and compared across datasets. Next, transmissibility along each axis (span, flap, edge) is computed to quantify how vibration energy propagates from the tip to the root; reductions in transmissibility may indicate stiffness loss or early-stage damage.

While these methods provide strong qualitative insight, quantitative structural evaluation requires Operational Modal Analysis (OMA) using Frequency Domain Decomposition (FDD) to identify changes in natural frequencies, damping, and mode shapes key indicators of stiffness degradation and damage progression. To further evaluate subtle damage mechanisms such as crack propagation, which may not be externally observable, the vibration data is analysed using Stochastic Subspace Identification (SSI), enabling accurate estimation of damping ratios and modal parameters under operational loads. The analysis concludes with engineering recommendations for the client based on the combined time, frequency, and modal domain findings.

Forces Governing Blade Dynamics

F_D = Drag force acting on the blade, F_L = Lift force acting on the blade, F_a = Net axial force acting on the blade, F_e = Net forces acting in the plane of rotation, F_f = Net forces acting perpendicular to the plane of rotation, α = Angle of Attack.

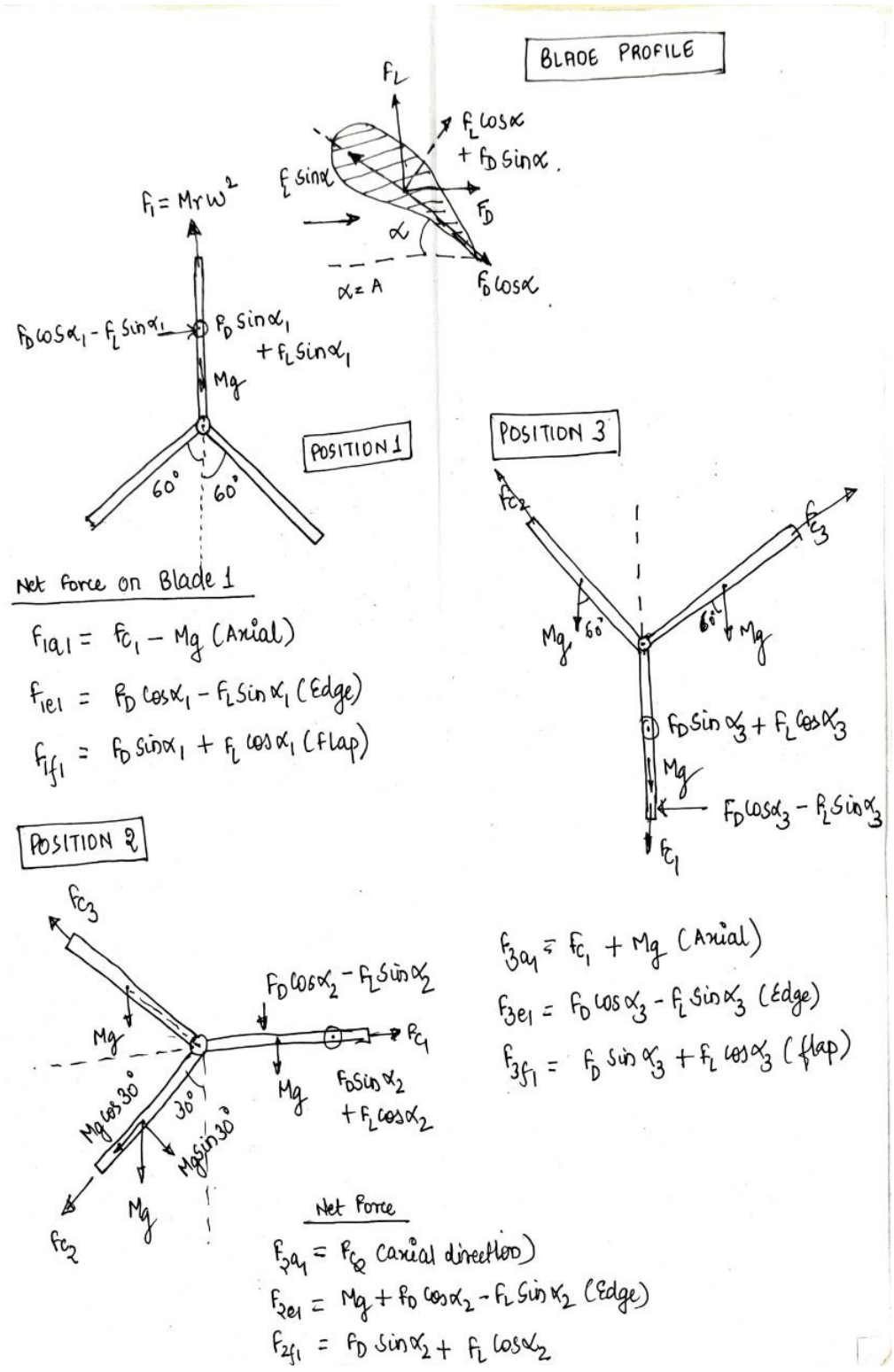

Figure 1: Aerodynamic forces and resultant components acting on a wind turbine blade.

Time Domain Analysis

The analysis begins with descriptive statistics for each vibration channel, including mean, RMS, standard deviation, higher-order statistics, and peak-based factors. These metrics characterise overall vibration energy, variability, impulsiveness, and deviations from normal behaviour, providing early indications of loading changes, aerodynamic imbalance, or emerging structural faults. Together, they establish a baseline understanding of the blade's dynamic response and help identify abnormal patterns before advancing to frequency-domain or modal analysis.

A comparison of the time-domain statistical features between Turbine 1 (T1) and Turbine 2 (T2) shows consistent and technically meaningful deviations across nearly all sensors and measurement directions. T2 exhibits higher RMS and standard deviation values on most channels, particularly in the flapwise and edgewise tip locations, indicating increased broadband vibrational energy and greater overall dynamic response amplitudes compared to T1. Several impulsiveness-related metrics, including crest factor, impulse factor, clearance factor, and margin factor, are systematically elevated in T2, with some channels showing significantly higher values (e.g., crest factors approaching or exceeding 3, margin factors >4). Such increases usually happen when the blade is exposed to stronger short-term loads, has become less stiff, or is experiencing occasional large vibration spikes.

The dominant frequency remains essentially unchanged between T1 and T2, with values clustered around 0.206–0.218 Hz, indicating that the global 1P response and the first bending mode of the blades are stable. This suggests that there has been no major change in overall blade stiffness, boundary conditions, or rotor speed between the two measurement periods. However, the dominant amplitude shows a consistent and noticeable increase in T2 across most channels compared with T1. This rise in vibration energy may reflect higher operational loading, such as increased wind speed or early-stage stiffness degradation, which can amplify blade deflection without significantly shifting the natural frequency.

Additionally, the envelope kurtosis, which is sensitive to non-Gaussian or damage-driven vibration signatures, is consistently higher at multiple locations in T2, reinforcing the presence of more pronounced impulsive or non-linear vibrational behaviour. In contrast, mean and skewness values differ only slightly between turbines, suggesting that baseline loading conditions and sensor biases remain comparable. Overall, the systematically elevated amplitude-related, impulsiveness-related, and envelope-based statistics in T2 align strongly with the later PSD and modal analysis results. Taken together, these indicators provide persuasive evidence that T2's blades are experiencing increased vibrational excitation and reduced structural stiffness or increased damping, with the greatest effects occurring in flapwise and tip measurements, where changes in stiffness produce the most pronounced dynamic impact.

Frequency Domain Analysis

A comparison of the Welch Power Spectral Density (PSD) plots for Blade 2 on Turbine 1 and Turbine 2 reveals a consistent and systematic increase in vibration energy across all measured directions, edge, span, and flap and at both the root and tip of the blade. Under identical operating conditions, as confirmed by the identical 1P rotor-frequency line, Turbine 2 exhibits broadband PSD amplitudes that are significantly higher than those of Turbine 1 from approximately 1 Hz to 30 Hz. This effect is most pronounced in the flapwise direction, where the PSD levels of Turbine 2 exceed those of Turbine 1 by up to an order of magnitude in the 5–15 Hz band, which is strongly influenced by the blade's primary bending modes. The tip sensors show these differences even more strongly, suggesting the vibration increases toward the blade tip. This points to a change in overall blade stiffness or mass, not a problem at the root or with a sensor.

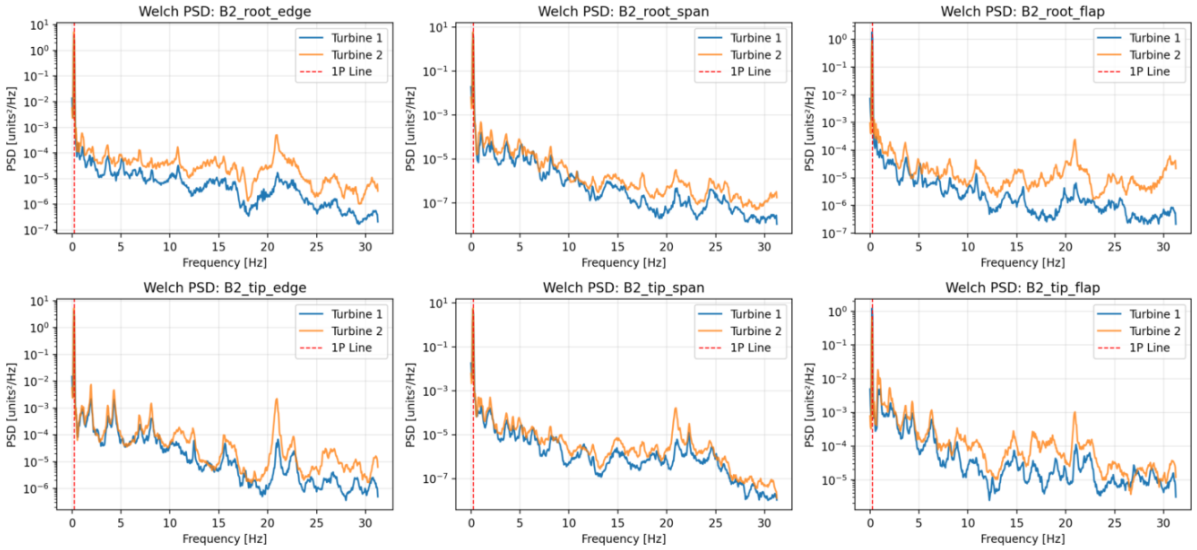

Figure 2: Welch Power Spectral Density Comparison for Blade 2

The PSD elevation observed in Turbine 2 across all three orthogonal directions, but especially in flapwise bending, provides strong evidence of reduced structural stiffness, increased effective mass, or increased damping relative to Turbine 1. This interpretation directly aligns with the modal analysis results, which showed a 20–25% reduction in the first flapwise natural frequency for all blades on Turbine 2. The combined frequency-domain and modal-domain indicators therefore point toward a turbine-wide change in dynamic characteristics likely arising from blade softening, moisture ingress, or deterioration of load-bearing laminate or pitch-root boundary stiffness. The PSD findings confirm that Turbine 2's blades are softer and show higher vibrations, suggesting the need for further inspection.

Coherence Analysis

Coherence quantifies the linear relationship between two vibration signals across frequency, making it a powerful indicator of structural continuity in wind turbine blades. In a healthy blade, which behaves as a continuous elastic beam, vibrations propagate cleanly

along the structure, resulting in high coherence between sensors, particularly between the root and tip in the same direction. Natural frequencies typically appear as coherence peaks, while unrelated degrees of freedom (e.g., edge vs. span) should show low coherence. When structural damage occurs, this continuity is disrupted, causing irregular, reduced, or unexpectedly elevated coherence patterns.

Across all sensor pairings for Blade B3, the coherence behaviour of Turbine 1 aligns well with expectations for a healthy blade. Root–root and root–tip pairs show coherence values near unity up to approximately 0.5–0.8 Hz, reflecting intact global bending behaviour. Beyond 1 Hz, coherence decreases smoothly with frequency and exhibits clear modal transitions. Cross-directional coherence (e.g., edge vs. span) remains low across the spectrum, confirming that the blade's degrees of freedom remain dynamically uncoupled as expected. Tip–tip interactions also show low or modest coherence except near modal frequencies, indicating that localised motion at the tip behaves independently and without abnormal coupling.

In contrast, Turbine 2 shows consistent structural irregularities across nearly all coherence pairings. Although low-frequency coherence remains high, indicating that global motion is still intact, coherence begins to drop noticeably earlier than in Turbine 1, particularly in root–tip pairs, where the decline often starts before 0.4–0.5 Hz. This early loss of coherence implies that bending waves do not propagate cleanly along the blade, a hallmark of mid-span stiffness reduction often associated with spar-cap cracking or shear-web delamination. Above 1 Hz, Turbine 2 displays irregular, fragmented coherence behaviour rather than the smooth modal structure observed in Turbine 1. These irregular dips and scattered coherence values point to disrupted load transfer along the blade's length.

The most striking deviations appear in the tip–tip and cross-directional pairings. Turbine 2 shows abnormally high coherence between unrelated degrees of freedom at the tip (e.g., tip-edge vs. tip-flap), particularly in the 10–18 Hz range. Such behaviour does not occur in the healthy blade and strongly indicates increased torsional–bending coupling. This

typically arises when stiffness is locally reduced near the trailing edge or spar cap, causing the tip region to move more uniformly across multiple directions. Additionally, several cross-directional root–tip pairings show elevated coherence only in Turbine 2, suggesting that damage-induced asymmetry or local delamination is altering the dynamic response.

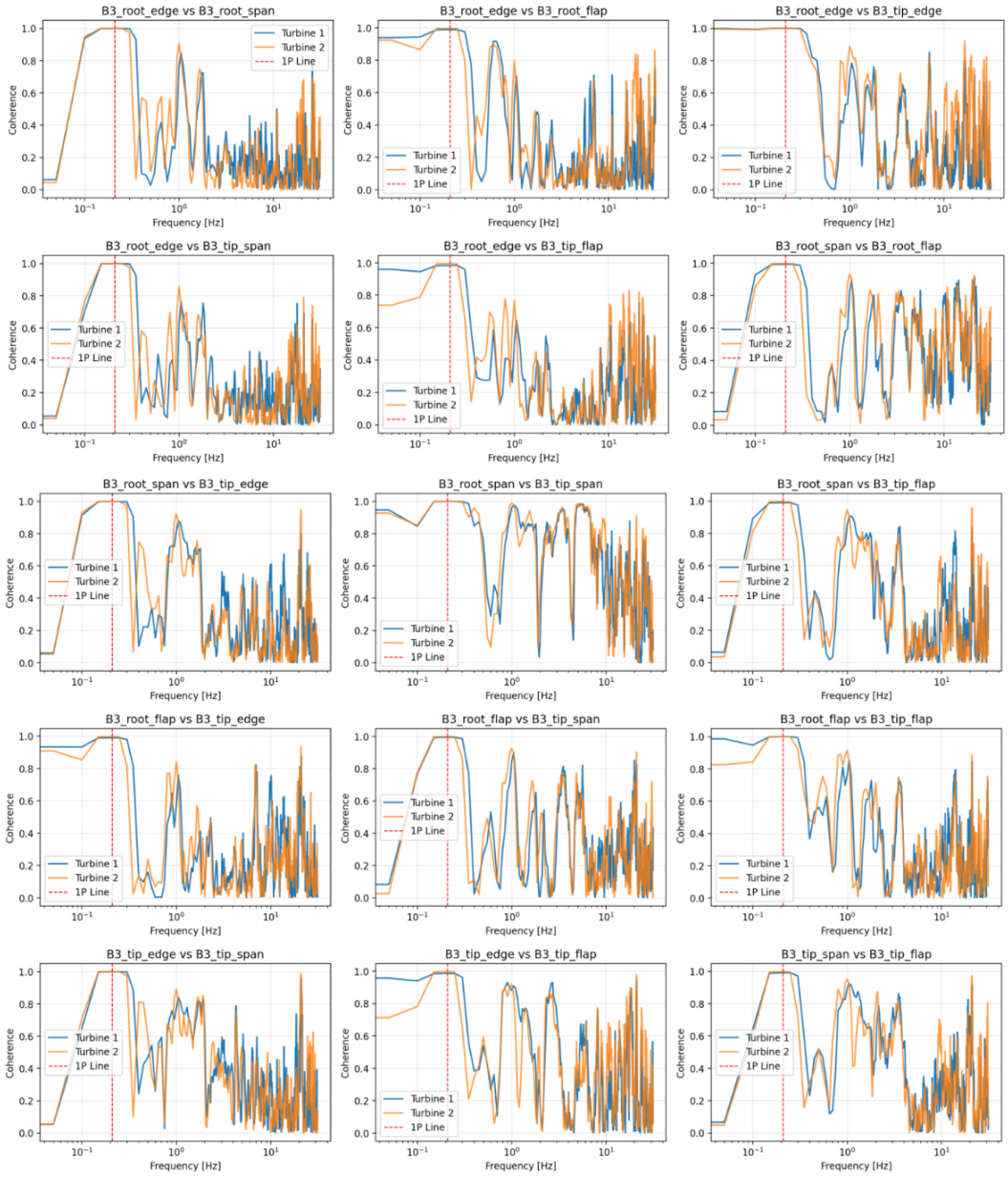

Figure 3: Coherence Analysis for Blade 3

Taken together, the coherence patterns provide robust evidence of structural degradation in Turbine 2's Blade B3. The early loss of root–tip coherence indicates impaired load-transfer efficiency along the span, while the abnormally high tip-level cross-direction coherence points to localised damage near the tip, characteristics commonly associated with spar-cap cracking, trailing-edge separation, or shear-web delamination. These findings are consistent with the increased transmissibility, PSD elevation, and modal-shape distortions observed in later analyses. Overall, the coherence analysis supports the conclusion that Turbine 2 exhibits significant stiffness loss and emerging structural damage, warranting targeted inspection through UAV imaging, thermography, or tap-testing.

Transmissibility

Transmissibility quantifies how vibration energy propagates along the blade and is defined as the ratio of the tip PSD to the root PSD for a given axis. It is a key structural health indicator in wind turbine analytics because it is highly sensitive to changes in bending and torsional stiffness, can reveal damage progression, and enables consistent comparison across time, operating conditions, and turbines. In the presented results, the increased vibration amplitude in the spanwise and flapwise directions suggests either higher aerodynamic loading or a reduction in blade stiffness. For Turbine 2, shown in orange, the sharper spectral peaks and changes in higher-mode shapes indicate possible tip-level damage, reflected in significantly elevated transmissibility.

The transmissibility plots also show that the global (first) mode remains relatively unchanged, while higher modes exhibit slight frequency reductions along with shoulder-like distortions or peak splitting, features commonly associated with localised stiffness loss such as foam-core delamination or degradation near the shear web. At the 1P rotational frequency, transmissibility values for the two turbines appear similar across all axes (edge, span, flap), but subtle deviations still imply that their load-transfer behaviour and modal characteristics are not perfectly matched, suggesting early or localized structural changes.

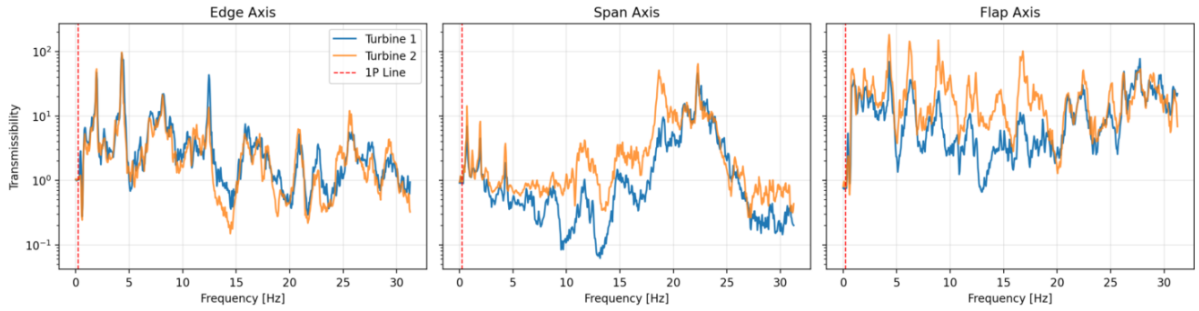

Figure 4: Transmissibility Analysis for Blade 1

For long-term monitoring, it is recommended that transmissibility be continually compared against an established baseline and that trends be analysed to detect gradual stiffness degradation or the onset of structural damage.

$$\Delta T(f) = \frac{T_{\text{current}}(f) - T_{\text{baseline}}(f)}{T_{\text{baseline}}(f)} \tag{0.0.1}$$

If a mode gets stronger without much frequency change, it could be due to higher excitation. But if this happens only on one blade and mainly in the flap direction, it likely means that the blade has lost stiffness near the tip or along the span.

Modal Analysis

The modal frequency table indicates a clear and technically meaningful difference in the dynamic behaviour of the two turbines. Across all three blades, Turbine 1 exhibits a consistent first flapwise natural frequency of approximately 1.05 Hz, whereas Turbine 2 shows a significantly reduced value of 0.8 Hz. A 20–25% drop in the first bending mode is highly diagnostic, as this mode is the most sensitive to global changes in blade stiffness, mass distribution, and root boundary conditions. Such a uniform reduction across all blades on Turbine 2 strongly suggests a system-level structural softening or mass increase, rather

than a localised defect affecting a single blade. Potential causes include material degradation, progressive laminate fatigue, reduced pitch bearing stiffness, accumulated moisture or water ingress inside the blades, or manufacturing differences leading to lower global stiffness.

Turbine_Blade	Mode 1	Mode 2	Mode 3	Mode 4	Mode 5	Mode 6	Mode 7	Mode 8
T1_B1	1.05	4.3	6.25	8.2	12.45	16.6	21.05	24.85
T2_B1	0.8	4.3	6.3	8.1	8.9	12.45	16.65	20.95
T1_B2	1.05	4.3	6.3	8.2	12.5	14.7	21.05	26.95
T2_B2	0.8	1.95	4.3	6.3	8.1	14.65	16.6	20.95
T1_B3	1.05	4.3	6.25	8.15	14.75	19	21.05	28.7
T2_B3	0.8	1.95	4.3	6.25	8.1	14.6	16.45	20.95

Figure 5: Frequency Domain Decomposition for Turbine 1 and 2

Higher-order modes (Modes 2–8) also show deviations between T1 and T2, although less uniformly. Some modes remain closely aligned, while others, particularly Modes 2 and 5, show noticeable reductions for Turbine 2. This mixed behaviour indicates that changes are not confined to a single frequency band but may arise from a broader alteration in the stiffness distribution along the blade span, affecting both lower and mid-order bending shapes. Importantly, the pattern is consistent across all blades of Turbine 2, which points away from isolated damage and instead toward a systematic shift in dynamic properties at the turbine or blade-family level.

Overall, the modal comparison provides compelling evidence that Turbine 2's blades exhibit reduced structural stiffness or increased effective mass, most pronounced in the first flapwise mode but observable across several higher modes as well. This should be looked into further, ideally by checking the operational data, pitch system, environmental conditions, and carrying out a focused blade inspection to determine whether the issue is operational, manufacturing-related, or an early sign of structural damage.

The Stochastic Subspace Identification(SSI) modal analysis reveals a clear degradation in the dynamic behavior of the defective turbine compared with the healthy one. In the healthy turbine, the first six global modes cluster around 0.21–0.22 Hz with very low damping (0.0007–0.004), and the mode shapes show clean, symmetric root–tip patterns across edge, span, and flap directions, indicating a stiff, well-coupled blade–hub system with no disruption in load transfer. In contrast, the defective turbine exhibits a systematic reduction in natural frequencies, dropping by 7–8% for the first modes and up to 15–17% for Modes 5–6, together with a dramatic increase in damping (up to an order of magnitude), signaling added frictional losses associated with internal structural damage. The mode shapes of the defective turbine no longer preserve the symmetry seen in the healthy case: root–tip magnitudes diverge, flapwise components grow disproportionately, and span–edge coupling becomes distorted, revealing a breakdown of uniform bending behavior along the blade. This asymmetric deformation pattern and increased damping, especially in higher modes, strongly indicate a localised stiffness reduction, likely spar-cap cracking or bondline delamination in the mid-span to root region, rather than an operational effect, as both turbines were operating at the same speed. Overall, the SSI results give consistent and conclusive evidence of structural degradation on the defective turbine's blade.

Across all three blades, the Modal Assurance Criterion (MAC) analysis clearly shows increasing levels of deviation in Turbine 2 relative to the Turbine 1 reference. Blade 1 exhibits high MAC values (0.89–0.92), indicating that its mode shapes remain very similar to the healthy baseline and showing no sign of structural degradation. Blade 2 shows moderate reductions in MAC (0.59–0.72), suggesting a meaningful change in stiffness or mass distribution, likely caused by erosion, surface wear, pitch misalignment, or early-stage structural softening, but not yet indicative of severe damage. Blade 3, however, presents a critical anomaly: while Modes 1–2 show moderate deviation (0.73), Mode 3 collapses to a MAC value near zero, meaning the mode shapes are essentially orthogonal to the baseline. This represents a fundamental change in dynamic behaviour and is strongly associated

with a localized structural issue such as delamination, cracking, trailing-edge separation, water ingress, or root looseness. In summary, Blade 1 appears healthy, Blade 2 requires follow-up inspection, and Blade 3 demands urgent investigation, as its dynamic signature is consistent with significant structural or boundary-condition deterioration.

Conclusion

This study demonstrates the value of a structured, multi-domain vibration analysis framework for assessing wind turbine blade condition. The early data cleaning and preparation ensured that the signals entering the analysis were reliable and free from artefacts, allowing the subsequent steps to reflect true blade behaviour. Time–domain features provided a first indication of abnormal loading and changes in vibrational intensity, while frequency–domain methods such as Welch PSD highlighted how the distribution of energy across frequencies can reveal stiffness variations and evolving damage mechanisms. Coherence and transmissibility added a spatial dimension, showing how well vibration propagates along the blade and identifying disruptions in load transfer that are often invisible in single-point measurements. Finally, modal analysis using FDD, SSI, and MAC offered the most diagnostic insight by characterising how the underlying structural properties of the blades have changed over time. Together, these complementary techniques illustrate how a modern Blade CMS, when paired with advanced analytics, can detect subtle stiffness loss, identify emerging defects, and guide targeted inspections long before failure becomes critical. This integrated approach provides a robust foundation for condition-based maintenance and long-term asset reliability.